

ImageNomer: developing an fMRI and omics visualization tool to detect racial bias in functional connectivity

Anton Orlichenko^a, Grant Daly^b, Anqi Liu^c, Hui Shen^c, Hong-Wen Deng^c, and Yu-Ping Wang^a

^aDepartment of Biomedical Engineering, Tulane University, New Orleans, LA, USA

^bCollege of Medicine, University of South Alabama, Mobile, AL, USA

^cSchool of Medicine, Tulane University, New Orleans, LA, USA

ABSTRACT

It can be difficult to identify trends and perform quality control in large, high-dimensional fMRI or omics datasets. To remedy this, we develop ImageNomer, a data visualization and analysis tool that allows inspection of both subject-level and cohort-level features. The tool allows visualization of phenotype correlation with functional connectivity (FC), partial connectivity (PC), dictionary components (PCA and our own method), and genomic data (single-nucleotide polymorphisms, SNPs). In addition, it allows visualization of weights from arbitrary ML models. ImageNomer is built with a Python backend and a Vue frontend. We validate ImageNomer using the Philadelphia Neurodevelopmental Cohort (PNC) dataset, which contains multitask fMRI and SNP data of healthy adolescents. Using correlation, greedy selection, or model weights, we find that a set of 10 FC features can explain 15% of variation in age, compared to 35% for the full 34,716 feature model. The four most significant FCs are either between bilateral default mode network (DMN) regions or spatially proximal subcortical areas. Additionally, we show that whereas both FC (fMRI) and SNPs (genomic) features can account for 10-15% of intelligence variation, this predictive ability disappears when controlling for race. We find that FC features can be used to predict race with 85% accuracy, compared to 78% accuracy for sex prediction. Using ImageNomer, this work casts doubt on the possibility of finding unbiased intelligence-related features in fMRI and SNPs of healthy adolescents.

Keywords: fMRI, functional connectivity, omics, interpretability, software, SNPs, PNC, normal development, intelligence, race, bias

1. INTRODUCTION

Functional magnetic resonance imaging (fMRI) uses the blood oxygen-level dependent (BOLD) signal to identify regions of increased neural activity.¹ Functional connectivity (FC) is an fMRI-derived measure that quantifies the synchronization between BOLD signal in different regions of the brain.² It and similar measures have been used to predict age,³ sex,⁴ intelligence,⁵ and disease status.^{6,7} Similar measures applied to magnetoencephalography (MEG) have also been used for predicting age⁸ and sex.⁹ Genomics can be used to make predictions that are much more accurate than those based on fMRI.^{10,11} Use of the two modalities together may give superior results.¹²

The effect sizes being measured by fMRI studies are often very small. Many studies have used FC features to predict intelligence, explaining 10% of the variance in a population³ or achieving a small correlation with ground truth $\rho \approx 0.3$.¹³ We show that the FC feature to intelligence correlation, however, is not statistically significant, and find confounding effects on FC. For example, Bennet et al. found that many effects found as significant by standard analysis techniques are simply due to noise.¹⁴ High dimensionality of the data and small effect size is exacerbated by the small cohort sizes of most recent fMRI studies.¹⁵ The average reproducible size for an fMRI result was found to be around 36 subjects.¹⁶ Additionally, changes in either scanner parameters¹⁷ or preprocessing pipeline¹⁸ may result in large changes in FC or predictive capability.

Further author information: (Send correspondence to Anton Orlichenko)

Anton Orlichenko: E-mail: aorlichenko@tulane.edu

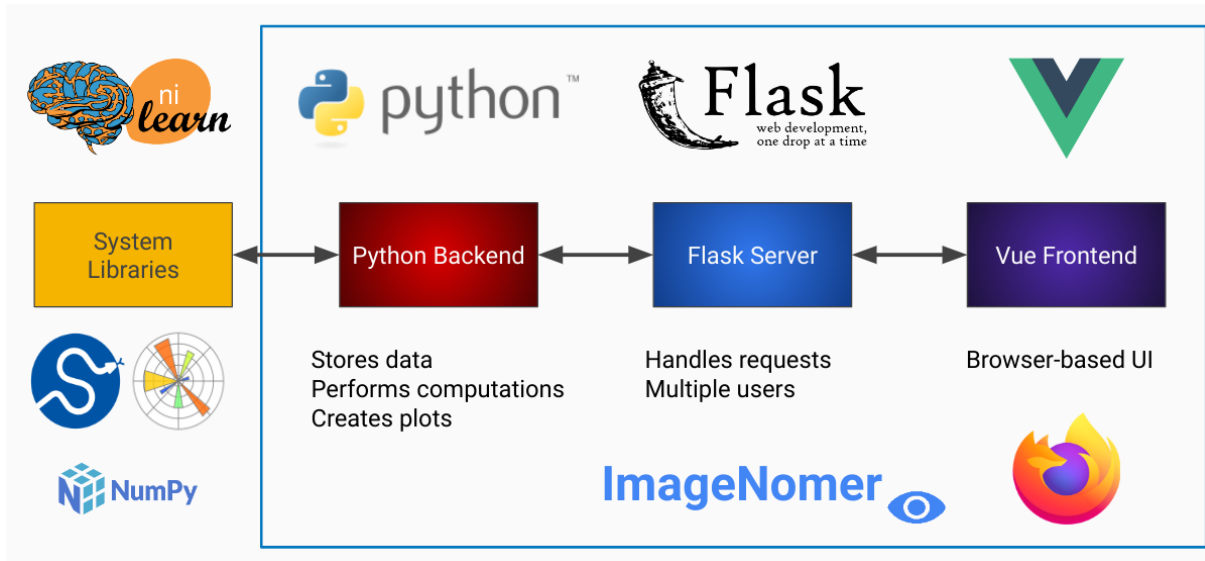


Figure 1. Overview of the ImageNomer architecture.

The same effect size problem is found in genome-wide association studies (GWAS). Although heritability for schizophrenia is around 80%,¹⁹ only 23% of variance can be explained by SNPs.²⁰ This is compared to age prediction on adolescents using fMRI, which can achieve 35% variance explained.³ Another issue is that most traits are highly polygenic. For instance, more than 2,000 genes have been identified as contributing factors to schizophrenia.²⁰ This means that a molecular basis for diseases ranging from autism²¹ to Alzheimer's²² is either partially or mostly lacking.

Many recent studies seek to fuse fMRI data with genomics for enhanced predictive power.¹² Canonical correlation analysis (CCA) or deep graph neural network (GNN) methods can effectively combine multiple modalities state of the art prediction.^{23,24} The interpretation of deep models, however, is an area of ongoing research, and is especially unclear in graphical models.²⁵ FC data may have tens of thousands of features per subject and there may be more than a million SNPs per dataset.²⁶

Correlation analysis can give a quick overview of the data, and subject-level or cohort-level views can be instrumental for quality control. We develop ImageNomer, a visualization and analysis tool for FC-based fMRI and omics. The tool allows for on-line correlation analysis as well as the comparison of features from outside models in a convenient GUI format. Additionally, we include the ability to analyze distribution of phenotypes. It is possible to view FC-based decompositions, e.g., PCA, and correlate their components with either SNPs or phenotypes. The code has been released and is available at the link in the footnote.*

2. METHODS

2.1 Architecture

ImageNomer is made up of three components (see Figure 1):

- a Python backend which integrates with available libraries such as matplotlib, scikit-learn, and Nilearn
- a Flask server that handles requests from the browser-based UI to the backend
- a Vue frontend which provides an interactive user experience from within the browser

*Available online at <https://github.com/TulaneMBB/ImageNomer>

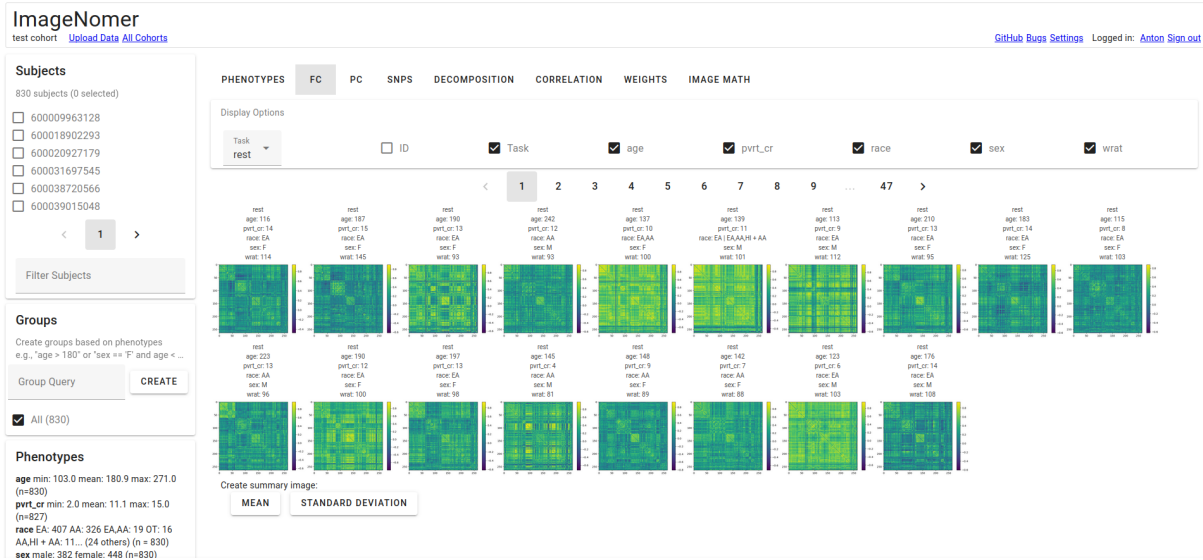


Figure 2. Main view of the ImageNomer program showing resting state FC for all subjects along with demographic data.

There is a web-based user interface that allows quick navigation around a cohort as well as the creation of summary graphs and correlation analyses. The main view is shown in Figure 2. Data is stored on a central server. The Python backend allows integration with standard libraries such as Nilearn, Scipy, Numpy, and Matplotlib. The Matplotlib backend is used to generate all graphs on the backend, which are sent to the frontend as images. The Vue frontend allows for modularity of UI components, provides a library of pre-built widgets via Vuetify, and provides a framework for interactivity.

2.2 Software features

ImageNomer has the following capabilities:

- Examine individual subject FC and PC
- Display trends in phenotypic features
- Correlate phenotypes with phenotypes, FC/PC features with phenotypes, or SNPs with phenotypes
- Display p-value maps for correlations
- Perform math on images
- Display components for FC decompositions (such as PCA)
- Correlate decomposition components with phenotypes or SNPs
- Display weights from machine learning models
- Summarize and average weights from multiple models

Future work with fMRI will likely require summarizing connectivity patterns into discrete network contributions.²⁷ Figure 3 illustrates finding correlation between individual network decompositions and phenotypic features.

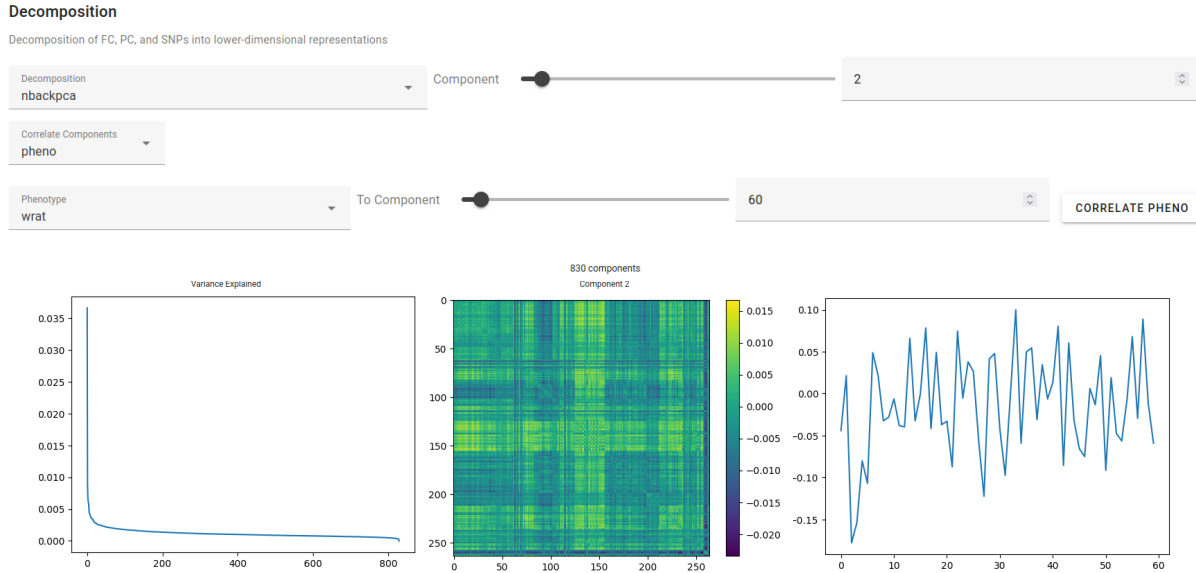


Figure 3. Correlation of PCA components with wide range achievement test (WRAT) score. The largest negative correlation component is displayed. Note the very low correlations.

2.3 Dataset

We tested ImageNomer by using it to examine the large PNC dataset.^{26,28} The PNC dataset contains fMRI scans, SNP information, cognitive batteries, questionnaires, and phenotype data from healthy adolescents between 8-23 years old. The dataset is enriched for European Ancestry (EA) and African Ancestry (AA) races. The PNC dataset contains fMRI scans for 1,445 healthy adolescents and SPN data for more than 9,267. We chose an 830-subject subset of the data which included subjects with SNP information as well as resting state (rest), working memory (nback), and emotion identification (emoid) scanner task fMRI scans. Intelligence is measured by Wide Range Achievement Test (WRAT) score²⁹ where the effect of age has been regressed out. The demographics of our study cohort are visualized in Figure 4.

2.3.1 fMRI

The scanner used was 3T Siemens TIM Trio whole-body scanner with a single-shot, interleaved multi-slice, gradient-echo, echo-planar imaging sequence. The voxel size was 3x3x3 mm and the image consisted of 46 slices. Scanning parameters were TR = 3000 ms, TE = 32 ms, and flip angle = 90 degrees. Gradient magnitude was 45 mT/m, with a maximum slew rate of 200 T/m/s. The resting state scan took 6.2 minutes (124 TR), the nback task took 11.6 minutes (231 TR), during which time adolescents performed the n-back memory task.³⁰ The emoid task took 10.5 minutes (210 TR), during which adolescents viewed faces displaying different emotions and identified which emotion was displayed.

fMRI from all tasks was deskulled, motion corrected, and registered into MNI space using the fmriprep software tool.³¹ The Power atlas³² was used to parcellate the brain into 264 5mm radius regions. The resulting BOLD time series were bandpass filtered between 0.01 and 0.15 Hz. FC and PC were calculated based on these time series.

2.3.2 SNPs

SNPs were collected using one of eight different platforms, with the largest set containing 1,185,051 SNPs.²⁶ For analysis, we selected a subset of 35,621 that were found in at least 50 subjects in the cohort. SNPs were categorized by haplotype as homozygous minor variant, heterozygous, and homozygous major variant. Missing values for subjects were set to zero for all haplotypes.

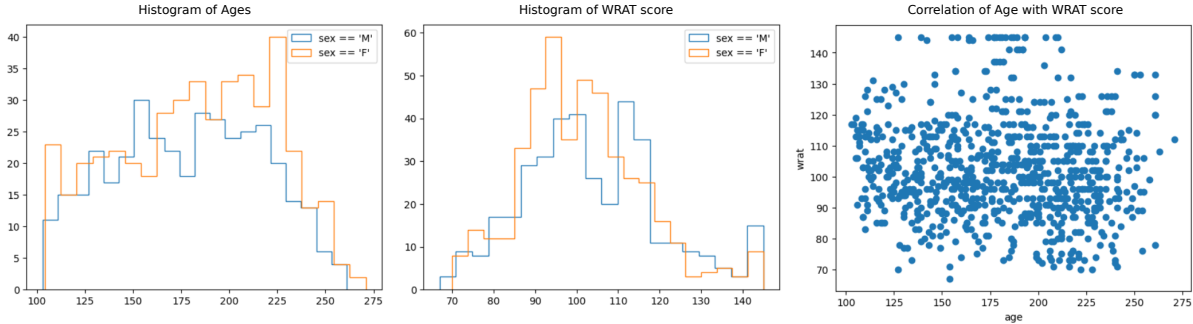


Figure 4. Demographics of our subset of the PNC dataset visualized using ImageNomer. Race distribution is visualized in later figures.

2.4 Feature selection

We investigate the ability of a small number of FC or SNP features to accurately predict age, intelligence, race, and sex. An 80% training set was used to estimate features, while a 20% test set was used for validation. For features estimated through ridge regression, logistic regression, or LASSO, random 80% subsets of the training set were selected 20 times, the model fit, and the resulting products of weights and features averaged.

Features were selected using correlation, model weights, and greedy selection. Correlation used simple Pearson correlation to rank features based on absolute value (Equation 1). Greedy feature selection³ fit a model one feature at a time based on correlation with the residual error on the training set.

$$\rho = \sigma_{xy}^2 / \sqrt{\sigma_{xx}^2 \sigma_{yy}^2} \quad (1)$$

3. RESULTS

We present results for age, intelligence, race, and sex prediction using FC and SNPs, as well as top feature selection. We find that, in our dataset, there are no unbiased predictors of intelligence among either FC or SNP features. Prediction results are summarized in Table 3.

Prediction	Modality	Metric	Null Model	Best Full Model	Best 10 Features
Age	FC	RMSE, months	38.4	26	32.2
Intelligence	FC	RMSE, WRAT score	15.1	13.6	15.1
Intelligence	SNPs	RMSE, WRAT score	15.1	14	-
Intelligence (AA)	FC	RMSE, WRAT score	13.9	13.8	13.9
Intelligence (AA)	SNPs	RMSE, WRAT score	13.9	13.4	-
Intelligence (EA)	FC	RMSE, WRAT score	14	14.1	14
Intelligence (EA)	SNPs	RMSE, WRAT score	14	13.6	-
Race	FC	Accuracy	58%	85%	72%
Sex	FC	Accuracy	51%	78%	62%

Table 1. Summary of prediction results for full models (34,716 features for FC, 35,621 features for SNPs) and top 10 feature models. Top 10 features selected on the training set. Statistically significant results are shown in bold.

3.1 Age features

Predicting the average of the age training dataset yields a null model RMSE of 38.4 months. In contrast, the best full 34,716-feature models yield an RMSE of 26-28 months for any of the three scanner tasks (see Figure 5). Selecting the top 10 features yields an explanation of 50% of the full model when using both raw FC data and with PCA. Most features vary between different scanner tasks and feature selection techniques, but several

appear repeatedly (see Figure 6). The regions are described in Table 3.1. It is noteworthy that the connections are between regions that are either bilaterally symmetric or, in three out of the four FCs, between spatially proximal regions. This gives support for the use of ReHO as a processing metric applied to fMRI.³³

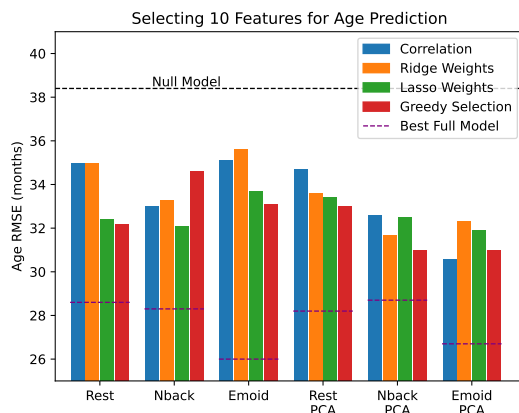


Figure 5. Selecting 10 out of 34,716 FC features for age prediction yields half of the predictive accuracy of the full model. There is no difference in predictive power between features selected by correlation, ridge regression, LASSO regression, or greedy feature selection. Ridge and LASSO weights are weighted over 20 runs. Features identified on training set and validated on test set.

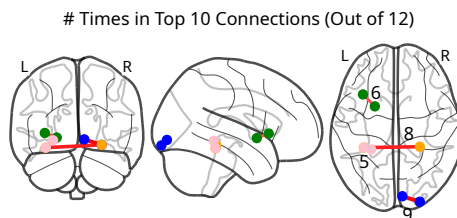


Figure 6. Top FCs from age feature selection. Numbers indicate how many times the FC showed up in correlation, ridge, LASSO, or greedy features for rest, nback, and emoid scanner tasks. Regions either bilateral symmetric or regionally proximal.

Region 1	Region 2	Power ROIs	FNs	# Times in Top 10 (/12)
Inferior Occipital Gyrus	Lingual Gyrus	238-252	UNK-UNK	9
Parahippocampa Gyrus	Fusiform Gyrus	112-113	DMN-DMN	8
Extra-Nuclear	Lentiform Nucleus	187-205	SAL-SUB	6
Parahippocampa Gyrus	Fusiform Gyrus	111-113	DMN-DMN	5

Table 2. Consensus of the most important regions for age prediction, which can explain up to 20% variation in age. FN=Functional Network, UNK=Uncertain, DMN=Default Mode Network, SAL=Saliency, SUB=Subcortical.

3.2 Intelligence features

Predicting the average of the training set yields a null model RMSE of 13.9 and 14 (WRAT score) for AA race and EA race, respectively. Using the full set of FC features, the best model yield RMSEs of 13.8 and 14.1, respectively. No feature selection method was able to yield 10 features that improve the RMSE over the null model.

When combining AA and EA groups, the null model RMSE becomes 15.1 (WRAT score), and the full model is able to achieve an RMSE of 13.6. Top 10 feature selection, however, was not successful.

Using the large set of SNPs, we are able to achieve an RMSE of 13.4 in the AA group and 13.6 in the EA group. Top 10 feature selection was not able to achieve an RMSE greater than the null model. Using LASSO identifies a few significant features (see Figure 7). The LASSO model, however, always yielded an RMSE worse than the null model.

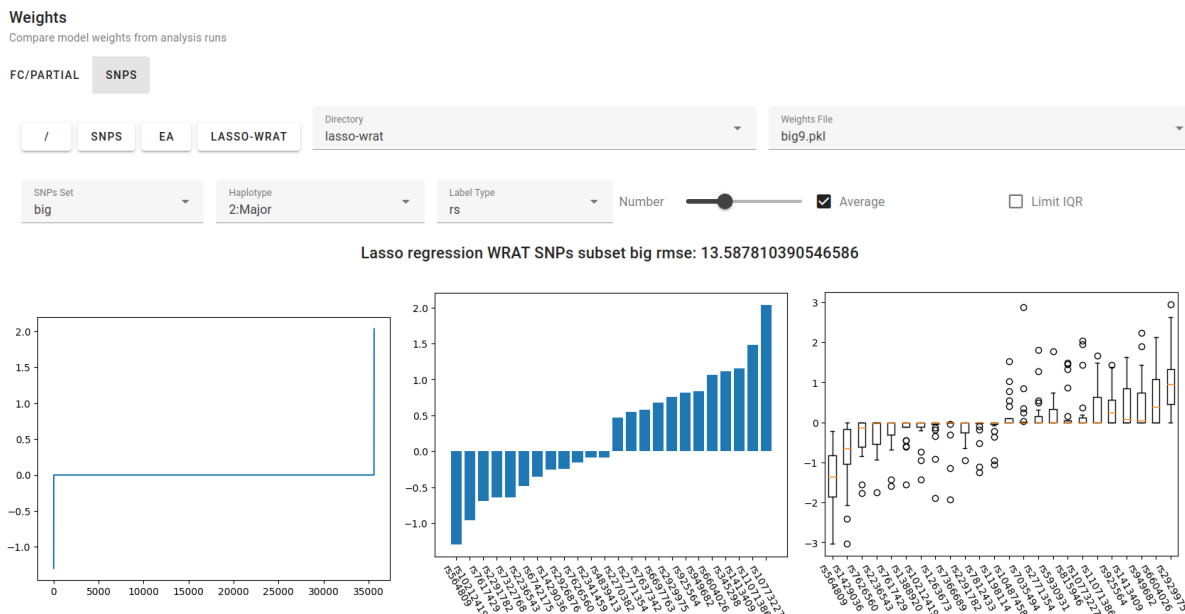


Figure 7. Average weights for intelligence prediction using SNPs from European American descent. Average of 20 runs of a LASSO model. Only several SNPs are selected with non-zero weight over all training set randomizations.

Combining the EA and AA groups, SNPs can yield an RMSE of 14 compared to the 15.1 RMSE of the null model. While combining groups doubles the size of the training set, any SNPs selected by the full group have a large distribution difference between EA and AA races. We can see a large difference in WRAT score between the EA and AA races (see Figure 8). SNPs, as genomic information, can easily detect race in our dataset, but we find that FC can as well.

3.3 Race features

FC features can be used to predict race with 85% accuracy in a Logistic Regression model, compared 58% accuracy for the null model. Top 10 feature selection can achieve an accuracy of 69-73%, although the features selected were different for different scanner tasks (emoid or rest).

It is unlikely that race prediction was instead predicting age, sex, or intelligence. As seen in Figure 9, the bias in age between races is much smaller than the bias in WRAT score. This can be seen in Figure 10. We see that raw FC to race correlation is much more significant than FC to WRAT correlation. The range of correlation for FC to WRAT is the same as for SNP to age, which we expect to be completely spurious. Indeed, it was impossible to successfully predict age from SNPs with any model.

3.4 Sex features

FC features can be used to predict sex with 78% accuracy in a Logistic Regression model, compared 58% accuracy for the null model. Top 10 feature selection can achieve an accuracy of 53-62%, although the features selected were different for different scanner tasks.

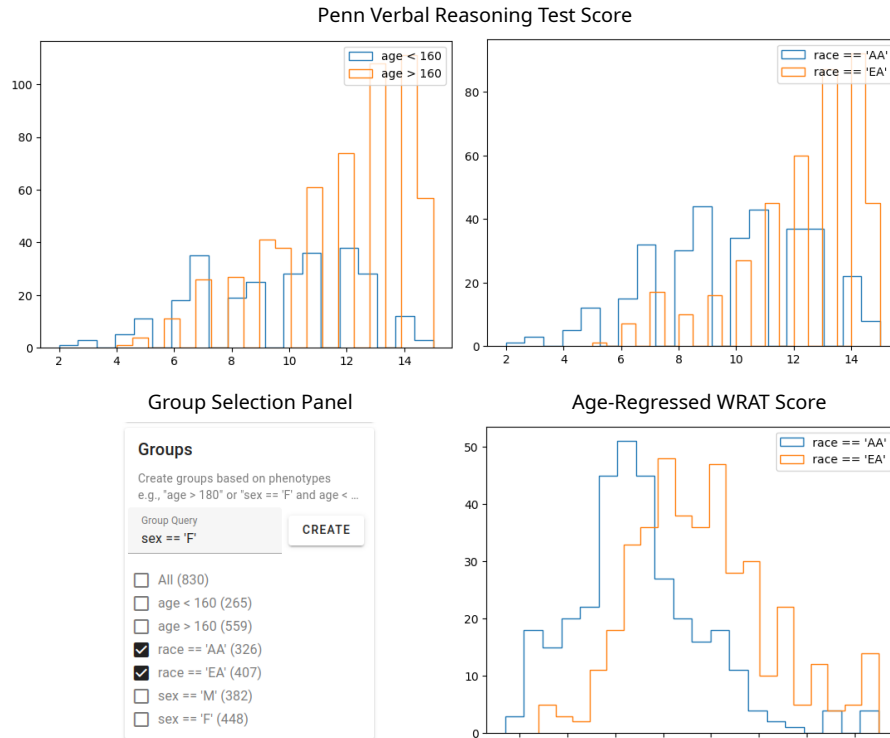


Figure 8. Examining dataset bias using ImageNomer. We find whereas age has been regressed from WRAT score, there is still a large racial bias. The PVRT score has been adjusted for neither age nor race and straightforward analysis may be problematic.

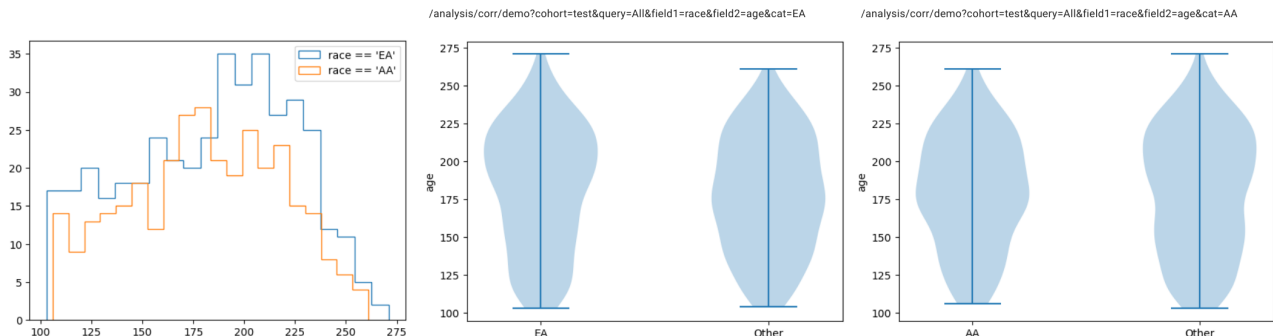


Figure 9. There is a much smaller dataset bias of race versus age compared to race versus WRAT. Quick examination by ImageNomer can reveal such differences. Age in months.

4. DISCUSSION

We present ImageNomer, a new fMRI and omics visualization and analysis tool. We use this tool to examine the large PNC dataset and discover features important for phenotype prediction. We find that 10 features give the majority of information required for age prediction. Sex and race can be moderately well predicted by FC features, with 10 FC features giving up to 72% race prediction accuracy, compared with 85% for the full model. Although not discussed, SNPs can predict sex and race perfectly, due to the presence of sex chromosome SNPs or race-related SNP distributions, respectively.

We find both FC features and SNPs can predict intelligence, as measured by WRAT score, but that this is probably due to a race confound, which is likely related to socio-economic status. When controlling for race,



Figure 10. We find that the range of correlations between WRAT and FC is similar to the range of correlations between age and SNPs, two sets of features that should be independent. On the other hand, correlation between European descent and FC is much larger, and gives much better prediction results.

FC-based prediction drops to the same as the null model and the SNP-based prediction becomes statistically insignificant. We find that there is a very low unconfounded effect of either SNPs or FC features on intelligence, if one exists at all.

ACKNOWLEDGMENTS

The authors would like acknowledge the NIH (grants R01 GM109068, R01 MH104680, R01 MH107354, P20 GM103472, R01 REB020407, R01 EB006841, R56MH124925) and NSF (#1539067) for partial funding support.

fMRI, SNP, and phenotype data came from the Neurodevelopmental Genomics: Trajectories of Complex Phenotypes database of genotypes and phenotypes repository, dbGaP Study Accession ID phs000607.v3.p2.

Part of the work on ImageNomer was conducted at the UBRITE Multiomics Hackathon[†] sponsored by the University of Alabama at Birmingham. The authors would like to acknowledge the organizers and mentors at UAB for their help in fostering teamwork and innovation in the bioinformatics community.

REFERENCES

- [1] Belliveau, J. W., Kennedy, D. N., McKinstry, R. C., Buchbinder, B. R., Weisskoff, R. M., Cohen, M. S., Vevea, J. M., Brady, T. J., and Rosen, B. R., “Functional mapping of the human visual cortex by magnetic resonance imaging,” *Science* **254** **5032**, 716–9 (1991).
- [2] Greicius, M. D., Krasnow, B., Reiss, A. L., and Menon, V., “Functional connectivity in the resting brain: A network analysis of the default mode hypothesis,” *Proceedings of the National Academy of Sciences* **100**(1), 253–258 (2003).

[†]<https://hackathon.ubrite.org/>

- [3] Orlichenko, A., Qu, G., Zhang, G., Patel, B., Wilson, T. W., Stephen, J. M., Calhoun, V. D., and Wang, Y.-P., “Latent similarity identifies important functional connections for phenotype prediction,” *IEEE Transactions on Biomedical Engineering*, 1–12 (2022).
- [4] Zhang, X., Liang, M., Qin, W., Wan, B., Yu, C., and Ming, D., “Gender differences are encoded differently in the structure and function of the human brain revealed by multimodal mri,” *Frontiers in Human Neuroscience* **14** (2020).
- [5] Qu, G., Xiao, L., Hu, W., Wang, J., Zhang, K., Calhoun, V. D., and ping Wang, Y., “Ensemble manifold regularized multi-modal graph convolutional network for cognitive ability prediction,” *IEEE Transactions on Biomedical Engineering* **68**, 3564–3573 (2021).
- [6] Du, Y., Fu, Z., and Calhoun, V. D., “Classification and prediction of brain disorders using functional connectivity: Promising but challenging,” *Frontiers in Neuroscience* **12** (2018).
- [7] Millar, P. R., Luckett, P. H., Gordon, B. A., and Benzinger, T. L., “Predicting brain age from functional connectivity in symptomatic and preclinical alzheimer disease,” *NeuroImage* **256**, 119228 (2022).
- [8] Xifra-Porxas, A., Ghosh, A., Mitsis, G. D., and Boudrias, M.-H., “Estimating brain age from structural MRI and MEG data: Insights from dimensionality reduction techniques,” *Neuroimage* **231**, 117822 (May 2021).
- [9] Ott, L. R., Penhale, S. H., Taylor, B. K., Lew, B. J., Wang, Y.-P., Calhoun, V. D., Stephen, J. M., and Wilson, T. W., “Spontaneous cortical MEG activity undergoes unique age- and sex-related changes during the transition to adolescence,” *Neuroimage* **244**, 118552 (Dec. 2021).
- [10] Krishnan, A., Zhang, R., Yao, V., Theesfeld, C. L., Wong, A. K., Tadych, A., Volfovsky, N., Packer, A., Lash, A., and Troyanskaya, O. G., “Genome-wide prediction and functional characterization of the genetic basis of autism spectrum disorder,” *Nat. Neurosci.* **19**, 1454–1462 (Nov. 2016).
- [11] Liu, Y., Xu, L., Li, J., Yu, J., and Yu, X., “Attentional connectivity-based prediction of autism using heterogeneous rs-fMRI data from CC200 atlas,” *Exp. Neurobiol.* **29**, 27–37 (Feb. 2020).
- [12] Hu, W., Meng, X., Bai, Y., Zhang, A., Qu, G., Cai, B., Zhang, G., Wilson, T. W., Stephen, J. M., Calhoun, V. D., and Wang, Y.-P., “Interpretable multimodal fusion networks reveal mechanisms of brain cognition,” *IEEE Trans. Med. Imaging* **40**, 1474–1483 (May 2021).
- [13] et al., U. P., “Optimising network modelling methods for fmri,” *NeuroImage* **211**, 116604 (2020).
- [14] Lyon, L., “Dead salmon and voodoo correlations: should we be sceptical about functional MRI?,” *Brain* **140**, e53 (Aug. 2017).
- [15] Szucs, D. and Ioannidis, J. P., “Sample size evolution in neuroimaging research: An evaluation of highly-cited studies (1990–2012) and of latest practices (2017–2018) in high-impact journals,” *NeuroImage* **221**, 117164 (2020).
- [16] Turner, B. O., Paul, E. J., Miller, M. B., and Barbey, A. K., “Small sample sizes reduce the replicability of task-based fMRI studies,” *Commun. Biol.* **1**, 62 (June 2018).
- [17] Saponaro, S., Giuliano, A., Bellotti, R., Lombardi, A., Tangaro, S., Oliva, P., Calderoni, S., and Retico, A., “Multi-site harmonization of MRI data uncovers machine-learning discrimination capability in barely separable populations: An example from the ABIDE dataset,” *NeuroImage Clin.* **35**, 103082 (June 2022).
- [18] DeSalvo, M. N., “Motion-dependent effects of functional magnetic resonance imaging preprocessing methodology on global functional connectivity,” *Brain Connect.* **10**, 578–584 (Dec. 2020).
- [19] Gejman, P. V., Sanders, A. R., and Duan, J., “The role of genetics in the etiology of schizophrenia,” *Psychiatr. Clin. North Am.* **33**, 35–66 (Mar. 2010).
- [20] Lee, S. H., The Schizophrenia Psychiatric Genome-Wide Association Study Consortium (PGC-SCZ), DeCandia, T. R., Ripke, S., Yang, J., Sullivan, P. F., Goddard, M. E., Keller, M. C., Visscher, P. M., Wray, N. R., The International Schizophrenia Consortium (ISC), and The Molecular Genetics of Schizophrenia Collaboration (MGS), “Estimating the proportion of variation in susceptibility to schizophrenia captured by common SNPs,” *Nat. Genet.* **44**, 247–250 (Mar. 2012).
- [21] Gill, P. S., Clothier, J. L., Veerapandiyam, A., Dweep, H., Porter-Gill, P. A., and Schaefer, G. B., “Molecular dysregulation in autism spectrum disorder,” *J. Pers. Med.* **11**, 848 (Aug. 2021).
- [22] Guo, T., Zhang, D., Zeng, Y., Huang, T. Y., Xu, H., and Zhao, Y., “Molecular and cellular mechanisms underlying the pathogenesis of alzheimer’s disease,” *Mol. Neurodegener.* **15**, 40 (July 2020).

- [23] Song, X., Li, R., Wang, K., Bai, Y., Xiao, Y., and Wang, Y.-P., “Joint sparse collaborative regression on imaging genetics study of schizophrenia,” *IEEE/ACM Trans. Comput. Biol. Bioinform.* **PP** (May 2022).
- [24] Wang, T., Shao, W., Huang, Z., Tang, H., Zhang, J., Ding, Z., and Huang, K., “MOGONET integrates multi-omics data using graph convolutional networks allowing patient classification and biomarker identification,” *Nat. Commun.* **12**, 3445 (June 2021).
- [25] Yuan, H., Yu, H., Gui, S., and Ji, S., “Explainability in graph neural networks: A taxonomic survey,” (2020).
- [26] Glessner, J. T., Reilly, M. P., Kim, C. E., Takahashi, N., Albano, A., Hou, C., Bradfield, J. P., Zhang, H., Sleiman, P. M. A., Flory, J. H., Imielinski, M., Frackelton, E. C., Chiavacci, R., Thomas, K. A., Garris, M., Otieno, F. G., Davidson, M., Weiser, M., Reichenberg, A., Davis, K. L., Friedman, J. I., Cappola, T. P., Margulies, K. B., Rader, D. J., Grant, S. F. A., Buxbaum, J. D., Gur, R. E., and Hakonarson, H., “Strong synaptic transmission impact by copy number variations in schizophrenia,” *Proc. Natl. Acad. Sci. U. S. A.* **107**, 10584–10589 (June 2010).
- [27] Wang, Z., Xin, J., Wang, Z., Yao, Y., Zhao, Y., and Qian, W., “Brain functional network modeling and analysis based on fMRI: a systematic review,” *Cogn. Neurodyn.* **15**, 389–403 (June 2021).
- [28] Satterthwaite, T. D., Elliott, M. A., Ruparel, K., Loughhead, J., Prabhakaran, K., Calkins, M. E., Hopson, R., Jackson, C., Keefe, J., Riley, M., Mentch, F. D., Sleiman, P. M. A., Verma, R., Davatzikos, C., Hakonarson, H., Gur, R. C., and Gur, R. E., “Neuroimaging of the philadelphia neurodevelopmental cohort,” *NeuroImage* **86**, 544–553 (2014).
- [29] Sayegh, P., Arentoft, A., Thaler, N. S., Dean, A. C., and Thames, A. D., “Quality of education predicts performance on the wide range achievement test-4th edition word reading subtest.,” *Archives of clinical neuropsychology : the official journal of the National Academy of Neuropsychologists* **29** **8**, 731–6 (2014).
- [30] Ragland, J. D., Turetsky, B. I., Gur, R. C., Gunning-Dixon, F. M., Turner, T. H., Schroeder, L., Chan, R. M., and Gur, R. E., “Working memory for complex figures: an fmri comparison of letter and fractal n-back tasks.,” *Neuropsychology* **16** **3**, 370–9 (2002).
- [31] Esteban, O., Blair, R., Markiewicz, C. J., Berleant, S. L., Moodie, C., Ma, F., Isik, A. I., Erramuzpe, A., Goncalves, M., Poldrack, R. A., and Gorgolewski, K. J., “poldracklab/fmriprep: 1.0.0-rc5,” (Sept. 2017).
- [32] Power, J. D., Cohen, A. L., Nelson, S. M., Wig, G. S., Barnes, K. A., Church, J. A., Vogel, A. C., Laumann, T. O., Miezin, F. M., Schlaggar, B. L., and Petersen, S. E., “Functional network organization of the human brain,” *Neuron* **72**, 665–678 (2011).
- [33] Jiang, L. and Zuo, X.-N., “Regional homogeneity: A multimodal, multiscale neuroimaging marker of the human connectome,” *Neuroscientist* **22**, 486–505 (Oct. 2016).